Efficient Method for Calculating Kinetic Parameters Using T_1-Weighted Dynamic Contrast-Enhanced Magnetic Resonance Imaging

Kenya Murase*

It has become increasingly important to quantitatively estimate tissue physiological parameters such as perfusion, capillary permeability, and the volume of extravascular-extracellular space (EES) using T_1-weighted dynamic contrast-enhanced MRI (DCE-MRI). A linear equation was derived by integrating the differential equation describing the kinetic behavior of contrast agent (CA) in tissue, from which K_1 (rate constant for the transfer of CA from plasma to EES), k_2 (rate constant for the transfer from EES to plasma), and V_p (plasma volume) can be easily obtained by the linear least-squares (LLSQ) method. The usefulness of this method was investigated by means of computer simulations, in comparison with the nonlinear least-squares (NLSQ) method. The new method calculated the above parameters faster than the NLSQ method by a factor of approximately 6, and estimated them more accurately than the NLSQ method at a signal-to-noise ratio (SNR) of < ~10. This method will be useful for generating functional images of K_1, k_2, and V_p from DCE-MRI data. Magn Reson Med 51:858–862, 2004.

Key words: kinetic parameter estimation; dynamic contrast-enhanced MRI; linear least-squares method; nonlinear least-squares method; functional image

Dynamic contrast-enhanced magnetic resonance imaging (DCE-MRI) is the acquisition of serial MR images before, during, and after an intravenous administration of contrast agent (CA) (e.g., Gd-DTPA). This technique has become increasingly important for estimating tissue physiological parameters such as perfusion, capillary permeability, and the volume of extravascular-extracellular space (EES) (1,2). The revealed kinetics of wash-in and wash-out of CA are used to characterize masses as malignant or benign, and to determine whether a tumor is responding to therapy (1,2). Compared with methods involving the use of single photon emission computed tomography (SPECT) or positron emission tomography (PET), the quantification of physiological parameters by DCE-MRI offers several advantages, such as improved spatial resolution, no exposure of the patient to ionizing radiation, and the ability to combine morphological and functional information during a single imaging session (2).

Department of Medical Physics and Engineering, Division of Medical Technology and Science, Faculty of Health Science, Graduate School of Medicine, Osaka University, Osaka, Japan.

*Correspondence to: Kenya Murase, Dr. Med. Sci., Dr. Eng., Department of Medical Physics and Engineering, Division of Medical Technology and Science, Faculty of Health Science, Graduate School of Medicine, Osaka University, 1-7 Yamadaoka, Suita, Osaka 565-0871, Japan. E-mail: murase@sahs.med.osaka-u.ac.jp

Received 4 June 2003; revised 12 November 2003; accepted 14 November 2003.

DOI 10.1002/mrm.20022
Published online in Wiley InterScience (www.interscience.wiley.com).

Many investigators have proposed models for the quantification of physiological parameters using DCE-MRI. The three major models were originally proposed by Tofts and Kermode (3), Larsson et al. (4), and Brix et al. (5). To quantify the physiological parameters in terms of absolute values using DCE-MRI, the arterial input function (AIF) of the CA entering the tissue must be determined (6,7). For cases in which AIF is not directly assessed, the models proposed by Tofts and Kermode (3) and Brix et al. (5) have proved useful. However, when an artery runs through the imaged slices, the AIF can be obtained noninvasively from the arterial pixels (6,7). Although techniques to achieve this are not yet in common use, an increasing number of investigators are developing practical methods for doing so (6,7).

In general, kinetic parameters are estimated by model (curve) fitting with the nonlinear least-squares (NLSQ) method. However, the NLSQ method is not suitable for generating functional images of physiological parameters, because it is not efficient in terms of computation time. Thus, to generate functional images of physiological parameters by DCE-MRI, an efficient method for estimating kinetic parameters is necessary. Therefore, the purpose of this study was to demonstrate an efficient method for calculating kinetic parameters, and to investigate its usefulness using computer simulations in comparison with the NLSQ method.

MATERIALS AND METHODS

Pharmacokinetic Model

In this study, we adopted the commonly used pharmacokinetic model (2). This model assumes that the CA resides in and exchanges between two compartments in the tissue: the vascular space and EES. When this model is used, the differential equation describing the kinetic behavior of the CA in the tissue of interest is given by

$$\frac{dC_{tis}(t)}{dt} = K_1 \cdot C_p(t) - k_2 \cdot C_{tis}(t) \qquad [1]$$

where $C_{tis}(t)$ and $C_p(t)$ are the concentrations of the CA at time t in the tissue of interest and plasma, respectively, and K_1 and k_2 are the rate constants for the exchanges of CA between plasma and EES. In accord with a recent standardization (1), K_1 is given by $K_1 = F_p \cdot E$, where F_p is the plasma flow per unit volume of tissue, and E is the extraction fraction given by $E = 1 - e^{-PS/F_p}$, where PS is the capillary permeability-surface area product. k_2 is given by $k_2 = K_1/V_e$, where V_e is the distribution volume of CA in the EES per unit volume of tissue.

When the kinetic model includes a vascular term, Eq. [1] becomes (8)

$$\frac{d\lfloor C_{tis}(t) - V_p \cdot C_p(t)\rfloor}{dt} = K_1 \cdot C_p(t) - k_2 \cdot [C_{tis}(t) - V_p \cdot C_p(t)] \quad [2]$$

where V_p is the capillary plasma volume per unit volume of tissue. Solving Eq. [2] with the assumption that the initial conditions are zero yields

$$C_{tis}(t) = K_1 \cdot \int_0^t C_p(u) \cdot e^{-k_2 \cdot (t-u)} du + V_p \cdot C_p(t). \quad [3]$$

This equation has been used to analyze MR data in a number of studies (9).

Estimation of Kinetic Parameters

By fitting Eq. [3] to the concentration-time curve in the tissue acquired from DCE-MRI, one can estimate K_1, k_2, and V_p. In general, this can be performed by means of the NLSQ method. Thus, we call this approach the "NLSQ method." In practice, however, we used the simplex method (10) for minimization of function in this study. For minimization of function, several methods can be used, which are classified into two categories (10): 1) methods that require both function evaluations and derivatives, and 2) methods that require only function evaluations (and no derivatives). The simplex method is in the latter category, and thus it appears to be easier to implement than the methods in the first category. That is primarily why we adopted the simplex method for use in this study.

Alternatively, integrating both sides of Eq. [2] with the assumption that the initial conditions are zero (11), and expressing the result in a discrete form yield

$$C_{tis}(t_k) = (K_1 + k_2 \cdot V_p) \cdot \int_0^{t_k} C_p(u) du - k_2 \cdot \int_0^{t_k} C_{tis}(u) du + V_p \cdot C_p(t_k) \quad (k = 1,2,\cdots,n) \quad [4]$$

Equation [4] can be given in a matrix form as

$$\vec{C} = \vec{A} \cdot \vec{B} \quad [5]$$

where

$$\vec{A} = \begin{pmatrix} \int_0^{t_1} C_p(u) du & -\int_0^{t_1} C_{tis}(u) du & C_p(t_1) \\ \int_0^{t_2} C_p(u) du & -\int_0^{t_2} C_{tis}(u) du & C_p(t_2) \\ \vdots & \vdots & \vdots \\ \int_0^{t_n} C_p(u) du & -\int_0^{t_n} C_{tis}(u) du & C_p(t_n) \end{pmatrix},$$

$$\vec{B} = \begin{pmatrix} K_1 + k_2 \cdot V_p \\ k_2 \\ V_p \end{pmatrix},$$

and

$$\vec{C} = \begin{pmatrix} C_{tis}(t_1) \\ C_{tis}(t_2) \\ \vdots \\ C_{tis}(t_n) \end{pmatrix}.$$

When $C_{tis}(t_k)$ and $C_p(t_k)$ ($k = 1,2,\cdots,n$) are measured, Eq. [5] can be easily solved for the elements of $\vec{B}$ using the conventional linear least-squares (LLSQ) method, and finally K_1, k_2, and V_p can be easily obtained from the elements. We call this approach the "LLSQ method." In this study, we generated the elements of $\vec{A}$ by numerical integration using the trapezoidal rule (10).

Computer Simulation

To investigate the accuracy and robustness of the above methods against statistical noise, and the effect of the sampling interval, we performed computer simulations. First, the time-dependent concentration of AIF [$C_{AIF}(t)$] was modeled as a gamma-variate function (Γ) with a recirculation that consisted of a copy of Γ twice, that is,

$$C_{AIF}(t) = \Gamma(t,t_0,\alpha_0,\beta_0) + 0.2 \times \tilde{\Gamma}(t,t_1,\alpha_1,\beta_1) + 0.05 \times \tilde{\Gamma}(t,t_2,\alpha_2,\beta_2) \quad [6]$$

where Γ is defined as $\Gamma(t,t_0,\alpha_0,\beta_0) = (t - t_0)^{\alpha_0} \cdot e^{-(t-t_0)/\beta_0}$ ($t \geq t_0$) and $\tilde{\Gamma}$ is a gamma-variate function normalized such that the maximum is equal to that of Γ. The parameters used in this study were $t_0 = 32$ s, $T_1 = 60$ s, $t_2 = 90$ s, $\alpha_0 = \alpha_1 = \alpha_2 = 3.0$, $\beta_0 = 5$ s, $\beta_1 = 10$ s, and $\beta_2 = 20$ s. These parameters were selected to simulate the typical AIF obtained for quantitative measurement of tumor blood flow using DCE-MRI in patients with musculoskeletal tumors (12). Unless specifically stated, the sampling interval was taken as 1.6 s. It should be noted that the relationship between $C_{AIF}(t)$ and $C_p(t)$ is given by $C_{AIF}(t) = (1–Hct) \cdot C_p(t)$, where Hct is hematocrit. In this study, Hct was assumed to be 0.45.

Finally, the signal-time curve of AIF [$S_{AIF}(t)$] was obtained by $S_{AIF}(t) = S_0 + C_{AIF}(t)$, where S_0 denotes the precontrast (baseline) signal. In this simulation, S_0 was set to 50 (the typical baseline intensity of the AIF obtained in musculoskeletal imaging cited above (12)). Simulated signal-time curves were generated in the form of dynamic images (80 frames with a time step of 1.6 s). Then, Gaussian noise was added to give signal-to-noise ratios (SNRs) ranging from 5 to 100. The SNR was given by SNR = S_0/σ, where σ is the standard deviation (SD) of the noise generated from normally distributed random numbers with zero mean and unit variance, which was varied with SNR. When the kinetic parameters were estimated, $C_{AIF}(t)$ was obtained by subtracting the average intensity of the precontrast (baseline) signals from $S_{AIF}(t)$.

As in the simulation of AIF, the signal-time curve in the tissue of interest [$S_{tis}(t)$] was obtained by $S_{tis}(t) = S_0 +$

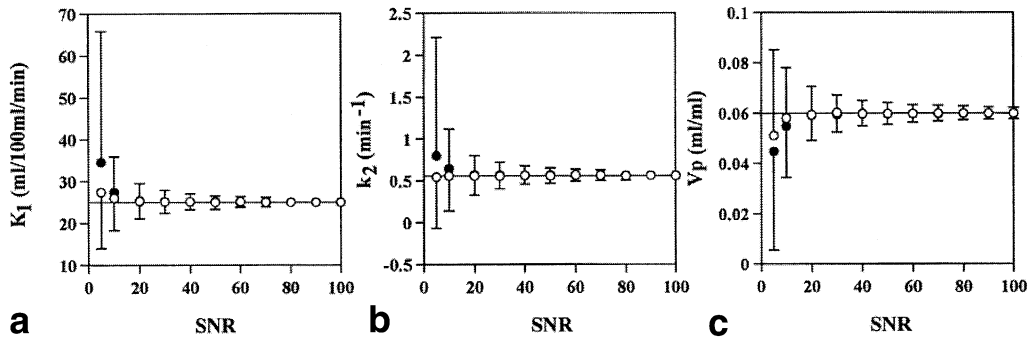

FIG. 1. Estimated values as a function of SNR when the true values for (**a**) K_1, (**b**) k_2, and (**c**) V_p are 25 ml/100 ml/min, 0.56 min^{-1}, and 0.06 ml/ml, respectively. The open circles show the mean values for the case in which the parameters were estimated by the linear least-squares (LLSQ) method, while the closed circles indicate the mean values obtained with the nonlinear least-squares (NLSQ) method. The horizontal lines represent the true values. The error bar represents the SD for 1000 simulations.

$C_{tis}(t)$, where $C_{tis}(t)$ is given by Eq. [3]. In this study, S_0 was taken to be the same as that in $S_{AIF}(t)$ for simplicity. Finally, Gaussian noise was added to give SNRs ranging from 5 to 100, as described above. When the kinetic parameters were estimated, $C_{tis}(t)$ was obtained by subtracting the average intensity of the precontrast (baseline) signals from $S_{tis}(t)$.

The kinetic parameters were assumed to be K_1 = 25 ml/100 ml/min, k_2 = 0.56 min^{-1}, and V_p = 0.06 ml/ml, which are representative of data previously acquired in a breast tumor (13). The K_1 and k_2 values were converted from the F_p, PS, and V_e values shown in Table 1 in Ref. 13 using the relations previously described. The values selected for V_p and V_e were based on estimates from the literature (13). The kinetic parameters adopted here will be acceptable for the purposes of this study.

We performed the simulations using Matlab (The MathWorks Inc., Natick, MA) on a Pentium 4 (2.8 GHz) with 2-GB RAM, and measured computation time using the functions "tic" and "toc" in Matlab.

Statistical Analysis

A Monte Carlo simulation of 1000 runs was performed for each condition. The mean and SD of the estimated K_1, k_2, and V_p values for 1000 runs were calculated. The accuracy of parameter estimation was evaluated in terms of root mean square error (RMSE) defined by $RMSE_i = \sqrt{\sum_{j=1}^{N}((\tilde{P}_{ij} - P_i)/P_i)^2/(N-1)} \times 100(\%)$, where $RMSE_i$, $\tilde{P}_{ij}$, P_i, and N are the RMSE of the ith parameter, the estimated value of the jth data of the ith parameter, the true value of the ith parameter, and the number of data (1000 in this study), respectively.

RESULTS

Figure 1 shows the estimated values of K_1 (a), k_2 (b), and V_p (c) as a function of SNR. In Fig. 1, the open circles show the mean values for the case in which the parameters were estimated by the LLSQ method, while the closed circles show the mean values obtained with the NLSQ method. The horizontal lines represent the true values, and the error bar represents the SD for 1000 simulations. Table 1 summarizes the results for RMSE. As shown in Fig. 1 and Table 1, the LLSQ method estimated the K_1, k_2, and V_p values more accurately than the NLSQ method at SNR $\leq$ 10. At SNR $>$ 10, the accuracy of the LLSQ method was almost the same as that of the NLSQ method.

Table 2 summarizes the results for RMSE for various sampling intervals. In these cases, SNR was assumed to be 10. As shown in Table 2, RMSE was improved by decreasing the sampling interval in both methods. The LLSQ method depended on the sampling interval in a manner similar to that of the NLSQ method.

Regarding computation time, the LLSQ method was faster than the NLSQ method by a factor of approximately 6 (15 s and 92 s for 1000 runs in the LLSQ and NLSQ

Table 1
Root Mean Square Error (RMSE) (%) of the K_1, k_2, and V_p Values Estimated Using the Linear Least-Squares (LLSQ) Method and the Non-linear Least-Squares (NLSQ) Method as a Function of Signal-to-Noise Ratio (SNR)

SNR	LLSQ method			NLSQ method		
	K_1	k_2	V_p	K_1	k_2	V_p
5	60.0	120.4	55.9	116.1	247.9	66.2
10	31.3	74.2	32.4	33.4	82.3	32.9
20	14.6	37.2	16.5	15.5	39.1	16.3
40	7.5	19.3	8.5	7.3	18.6	8.1
60	5.2	13.4	5.5	5.0	13.0	5.5
80	3.8	9.6	4.2	3.6	9.7	4.1
100	3.0	7.7	3.3	3.0	7.9	3.3

Table 2
RMSE (%) of the K_1, k_2, and V_p Values Estimated Using the LLSQ Method and the NLSQ Method as a Function of Sampling Interval at SNR = 10

Sampling interval (sec)	LLSQ method			NLSQ method		
	K_1	k_2	V_p	K_1	k_2	V_p
0.8	22.7	56.2	24.3	23.4	58.0	25.3
1.6	31.3	74.2	32.4	33.4	82.3	32.9
3.2	43.0	97.0	45.8	51.7	128.3	48.7

methods, respectively). For example, when parametric maps were generated with a 128 × 128 matrix on a pixel-by-pixel basis, the computation time was estimated to be approximately 4 min and 25 min for the LLSQ and NLSQ methods, respectively.

DISCUSSION

Many investigators have modeled the dynamic enhancement data that can be generated by T_1-weighted DCE-MRI after injection of a CA, such as Gd-DTPA (14). Most methods used to analyze DCE-MRI data employ compartment analysis to obtain some combination of the three principle parameters: the transfer constant (K^{trans}), the fractional volume of EES (V_e), and the rate constant (k_{ep}). k_{ep} is the ratio of K^{trans} to V_e. K^{trans} and k_{ep} correspond to K_1 and k_2 in this study, respectively.

In the model proposed by Tofts and Kermode (3), the plasma concentration after the injection of a bolus of Gd-DTPA was assumed to be the same as that measured in normal control subjects, which was fitted to a biexponential decay. In situations with no AIF and with limited temporal resolution, this model has proved useful. However, the use of a fixed AIF is known to introduce considerable error into the estimate of physiological parameters (15). The model proposed by Brix et al. (5) is one of several models that deal with the situation in which AIF is not directly assessed. Instead, the vascular space is assumed to be a perfect mixing chamber, with uniform concentration and a constant clearance rate (k_{el}) (5). The vascular concentration curve is assumed to be the result of a constant infusion of CA of known duration into the vascular space. This results in a mathematical expression for the extravascular-extracellular concentration in terms of three parameters: an amplitude parameter (A), k_{el}, and k_2.

As noted above, in this study we adopted the commonly used pharmacokinetic model (2). When this model is used, the concentration of the CA in the tissue of interest is given by Eq. [3]. To simulate data of a more realistic nature, a physiological model incorporating multiple parallel pathways and heterogeneous flow should be used (13). Recently, St. Lawrence and Lee (16) derived an equation describing the kinetic behavior of the tracer in a more realistic model. Their model offers the possibility of assessing the blood flow and extraction fraction or PS product simultaneously, but it may require carefully constrained supervised data fitting, additional measurements, or multiple tracers to overcome problems with parameter correlation (13). The choice of this model for data analysis requires a sampling interval less than the mean transit time of the tracer in the vascular space. When the sampling interval is equal to or greater than the mean transit time (on the order of a few seconds), this model may be simplified to a form similar to the model described by Eq. [3] (16). If an independent estimate of blood flow or capillary permeability is not essential, the model used in the present study may be an appropriate choice for analysis of DCE-MRI data (13).

In this study, we developed an efficient method for calculating kinetic parameters from T_1-weighted DCE-MRI data, and investigated its usefulness using computer simulations in comparison with the NLSQ method. Our results (shown in Fig. 1 and Table 1) suggest that the LLSQ method presented here is useful for kinetic analysis of CA in tissue by DCE-MRI.

To investigate the effect of statistical noise, we added Gaussian noise to the signal-time curves to generate SNRs ranging from 5 to 100. For typical clinical dynamic imaging, SNR appears to be in the lower end of this range, with single-pixel SNRs typically varying between 5 and 10. The fact that the LLSQ method can estimate the kinetic parameters faster and more accurately than the NLSQ method at SNR $< \sim$10 (Fig. 1 and Table 1) suggests that the LLSQ method can be used to generate functional images of kinetic parameters by applying it pixel by pixel. As noted above, we used the simplex method for minimization of function in the NLSQ method. This method does not use derivatives (10). This may be the main reason why the NLSQ method was inferior to the LLSQ method at low SNR (Fig. 1 and Table 1).

As shown in Table 2, the accuracy of the parameter estimations was improved by the use of shortened sampling intervals. A sensitivity-encoding (SENSE) technique was recently developed to enhance the performance of MRI by means of multiple receiver-coil arrays (17). This technique is expected to improve the temporal resolution. Thus, incorporating this technique would enhance the usefulness of the LLSQ method.

In conclusion, the LLSQ method can estimate the kinetic parameters from T_1-weighted DCE-MRI data faster than the NLSQ method, with no deterioration in accuracy. We believe this method will be useful for performing kinetic analyses of CA in tissue by DCE-MRI, and for generating functional images of kinetic parameters.

REFERENCES

1. Tofts PS, Brix G, Buckley DL, Evelhoch JL, Henderson E, Knopp MV, Larsson HBW, Lee T-Y, Mayr NA, Parker GJM, Port RE, Taylor J,

Weisskoff RM. Estimating kinetic parameters from dynamic contrast-enhanced T_1-weighted MRI of a diffusible tracer: standardized quantities and symbols. J Magn Reson Imaging 1999;10:223–232.
2. Choyke PL, Dwyer AJ, Knopp MV. Functional tumor imaging with dynamic contrast-enhanced magnetic resonance imaging. J Magn Reson Imaging 2003;17:509–520.
3. Tofts PS, Kermode AG. Measurement of the blood-brain barrier permeability and leakage space using dynamic MR imaging. I. Fundamental concepts. Magn Reson Med 1991;17:357–367.
4. Larsson HBW, Stubgaard M, Frederiksen JL, Jensen M, Henriksen O, Paulson OB. Quantitation of blood-brain barrier defect by magnetic resonance imaging and gadolinium-DTPA in patients with multiple sclerosis and brain tumors. Magn Reson Med 1990;16:117–131.
5. Brix G, Semmler W, Port R, Schad LR, Layer G, Lorenz WJ. Pharmacokinetic parameters in CNS Gd-DTPA enhanced MR imaging. J Comput Assist Tomogr 1991;15:612–628.
6. Fritz-Hansen T, Rostrup E, Larsson HBW, Sondergaard L, Ring P, Henriksen O. Measurement of the arterial concentration of Gd-DTPA using MRI: a step toward quantitative perfusion imaging. Magn Reson Med 1996;36:225–231.
7. Murase K, Kikuchi K, Miki H, Shimizu T, Ikezoe J. Determination of arterial input function using fuzzy clustering for quantification of cerebral blood flow with dynamic susceptibility contrast-enhanced MR imaging. J Magn Reson Imaging 2001;13:797–806.
8. Ohta S, Meyer E, Fujita H, Reutens DC, Evans A, Gjedde A. Cerebral [^{15}O]water clearance in humans determined by PET. I. Theory and normal values. J Cereb Blood Flow Metab 1996;16:765–780.
9. Fritz-Hansen T, Rostrup E, Sondergaard L, Ring RB, Amtorp O, Larsson HBW. Capillary transfer constant of Gd-DTPA in the myocardium at rest and during vasodilation assessed by MRI. Magn Reson Med 1998; 40:922–929.
10. Press WH, Teukolsky SA, Vetterling WT, Flannery BP. Numerical recipes in C. New York: Cambridge University Press; 1992.
11. Blomqvist G. On the construction of functional maps in positron emission tomography. J Cereb Blood Flow Metab 1984;4:629–632.
12. Sugawara Y, Murase K, Kikuchi K, Miki H, Ikezoe J, Sakayama K. Quantitative measurement of tumor blood flow using dynamic MRI and deconvolution analysis. Proceedings of the 88th Scientific Assembly and Annual Meeting of Radiological Society of North America. Radiology (Suppl) 2002;225(P):270.
13. Buckley DL. Uncertainty in the analysis of tracer kinetics using dynamic contrast-enhanced T_1-weighted MRI. Magn Reson Med 2002;47:601–606.
14. Tofts PS. Modeling tracer kinetics in dynamic Gd-DTPA MR imaging. J Magn Reson Imaging 1997;7:91–101.
15. Parker GJM, Tanner SF, Leach MO. Pitfalls in the measurement of tissue permeability over short time-scale using a low temporal resolution blood input function. In: Proceedings of the 4th Annual Meeting of ISMRM, New York, 1996. p 1582.
16. St. Lawrence KS, Lee TY. An adiabatic approximation to the tissue homogeneity model for water exchange in the brain. I. Theoretical derivation. J Cereb Blood Flow Metab 1998;18:1365–1377.
17. Pruessman KP, Weiger M, Scheidegger MB, Boesiger P. SENSE: sensitivity encoding for fast MRI. Magn Reson Med 1999;42:952–962.